JACS
JOURNAL OF THE AMERICAN CHEMICAL SOCIETY

COMMUNICATION

pubs.acs.org/JACS

# Rapid, Photoactivatable Turn-On Fluorescent Probes Based on an Intramolecular Photoclick Reaction

Zhipeng Yu, Lok Yin Ho, and Qing Lin*

Department of Chemistry, State University of New York at Buffalo, Buffalo, New York 14260-3000, United States

Supporting Information

**ABSTRACT:** Photoactivatable fluorescent probes are invaluable tools for the study of biological processes with high resolution in space and time. Numerous strategies have been developed in generating photoactivatable fluorescent probes, most of which rely on the photo-"uncaging" and photoisomerization reactions. To broaden photoactivation modalities, here we report a new strategy in which the fluorophore is generated in situ through an intramolecular tetrazole-alkene cycloaddition reaction ("photoclick chemistry"). By conjugating a specific microtubule-binding taxoid core to the tetrazole/alkene prefluorophores, robust photoactivatable fluorescent probes were obtained with fast photoactivation (~1 min) and high fluorescence turn-on ratio (up to 112-fold) in acetonitrile/PBS (1:1). Highly efficient photoactivation of the taxoid−tetrazoles inside the mammalian cells was also observed under a confocal fluorescence microscope when the treated cells were exposed to either a metal halide lamp light passing through a 300/395 filter or a 405 nm laser beam. Furthermore, a spatially controlled fluorescent labeling of microtubules in live CHO cells was demonstrated with a long-wavelength photoactivatable taxoid−tetrazole probe. Because of its modular design and tunability of the photoactivation efficiency and photophysical properties, this intramolecular photoclick reaction based approach should provide a versatile platform for designing photoactivatable fluorescent probes for various biological processes.

Photoactivatable small-molecule fluorescent probes have become an indispensable tool for microscopic studies of biomolecular dynamics in living cells, tissues, and animals.[1] Several strategies have been reported for the design of photoactivatable organic fluorophores, including reversibly photoactivatable fluorophores based on a light-induced bond-breaking and thermal bond-reforming process;[2] photo-uncaging of "caged" fluorophores such as fluorescein,[3] coumarin,[4] rhodamine,[5] and FRET-based dyes;[6] photorelease of fluorophores from quenchers via cleavage of the photolabile linkers;[7] and photoswitching of the spiropyran-merocyanine-based nanoparticles.[8] In these systems, the latent fluorophores are already in place, which may compromise the photoactivation efficiency due to the filtering effect.[9] Also, recent advance in the super-resolution microscopic techniques such as PALM[10] and STORM[11] also demands new strategies for designing photoactivatable fluorophores with increased biocompatibility, excellent turn-on efficiency, and greater flexibility in bioconjugation. An elegant example is the development of photoactivatable azido-DCDHF fluorophores by Moerner et al. that exhibit very high turn-on ratios in fluorescence (up to 1270-fold) and are suitable for super-resolution imaging of targeted proteins in live cells.[12]

We recently reported a bioorthogonal chemistry strategy for fluorescent labeling of proteins in live cells based on a photoinduced tetrazole-alkene cycloaddition reaction ("photoclick chemistry").[13] Fluorescent pyrazoline cycloadducts were formed after the reactions, ensuring that only alkene- or tetrazole-pretagged proteins were labeled. Because the cycloaddition rate was modest ($k_2$ values up to 10 $M^{-1}$ $s^{-1}$), relatively high concentrations of reagents (~100 $\mu$M) were typically required for labeling in the intracellular environment. For faster fluorescent labeling at reduced reagent concentrations, we reasoned that an intramolecular photoclick reaction of a prefluorophore containing both the tetrazole and the alkene functionalities would greatly increase the reaction rate, resulting in rapid turn-on fluorescence for more efficient protein visualization in vivo. To demonstrate this approach, we report the design, synthesis, and photophysical characterization of a class of ligand-directed, photoactivatable, turn-on fluorescent probes for the spatially controlled imaging of microtubules in live mammalian cells.

We decided to design turn-on fluorescent probes for imaging microtubules because (i) microtubules exhibit dynamic instability and are responsible for spatial organization and rapid remodeling of the cytoskeleton during cell division,[14] and (ii) specific microtubule-binding molecules such as paclitaxel[15] and its fluorescent derivatives[16] have been used in the study of microtubule motility in vivo. A series of taxoid−tetrazoles **1**−**4** were thus synthesized (Schemes S1−S4 in Supporting Information) in which 7-$\beta$-alanyltaxol core[17] is conjugated to the *para*-position of the *C*-phenyl ring of two water-soluble tetrazoles bearing an *o*-allyloxy group at *N*-phenyl ring via a variable flexible linker (Scheme 1). We expect that, upon photoirradiation, tetrazoles would undergo rapid cycloreversion reaction to generate reactive nitrile imine dipoles which spontaneously react with the prealigned allyl group to form the pyrazoline fluorophores. The substituted amines or amides on the *N*-phenyl ring and the various linkers at the *C*-phenyl ring serve to fine-tune the reactivity of the tetrazoles as well as the photophysical properties of the resulting pyrazoline fluorophores. To our satisfaction, nearly quantitative conversions for **1**−**4** were observed based on HPLC analysis of the reaction mixtures after photoirradiation using a 302 nm hand-held UV lamp (UVM, 0.16 AMPS, 2.3 mW/cm$^2$)[18] for 60−70 s (Figures S1−S4).

**Received:** May 24, 2011
**Published:** July 07, 2011





dx.doi.org/10.1021/ja204758c | *J. Am. Chem. Soc.* 2011, 133, 11912–11915

**Scheme 1. Design of Photoactivatable Turn-On Fluorescent Probes 1−4 for Microtubules Comprising of a 7-β-Alanyltaxol Core and a Tetrazole Prefluorophore Core**

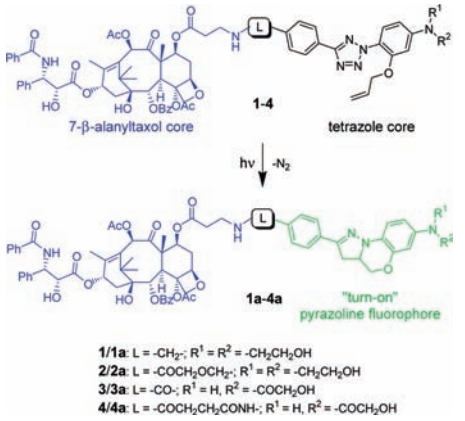


**Table 1. Photophysical Properties of the Taxoid−Pyrazolines and Fluorescence Turn-On Efficiency[a]**

| compound | $\lambda_{max}$ (nm)[b] | $\varepsilon$ ($M^{-1}$ $cm^{-1}$)[c] | $\varepsilon_{405}$ ($M^{-1}$ $cm^{-1}$)[d] | $\lambda_{em}$ (nm) | $\Phi_F$[e] | fluorescence turn-on[f] |
|---|---|---|---|---|---|---|
| **1** | 310 | 6400 | 460 | ND | ND | - |
| **1a** | 330 | 5100 | 2000 | 617 | 0.0024 | 21-fold |
| **1a**[g] | 340 | 4400 | 1600 | 580 | 0.036 | 34-fold |
| **2** | 311 | 12000 | 540 | ND | ND | - |
| **2a** | 332 | 8700 | 3000 | 614 | 0.0041 | 30-fold |
| **2a**[g] | 344 | 11600 | 4700 | 587 | 0.022 | 101-fold |
| **3** | 262[h] | 24400 | ND | ND | ND | - |
| **3a** | 358 | 12900 | 6900 | 584 | 0.034 | 111-fold |
| **4** | 276[h] | 30300 | ND | ND | ND | - |
| **4a** | 336 | 16400 | 3100 | 528 | 0.056 | 112-fold |

[a] Compounds were dissolved in ACN/PBS (1:1) to derive concentrations of 25 μM unless noted otherwise. [b] $\lambda_{max}$ in the 300−500 nm region. [c] Extinction coefficient at $\lambda_{max}$. [d] Extinction coefficient at 405 nm. [e] Quantum yields were measured using DAPI as a standard,[20] and integrated over 415−790 nm. [f] Obtained by comparing the emission intensity of taxoid−pyrazoline to that of the corresponding taxoid−tetrazole at $\lambda_{em}$; $\lambda_{ex}$ = 405 nm. [g] Dissolved in DCM. [h] $\lambda_{max}$ in the 250−500 nm region. ND = not detected.

To determine the magnitude of fluorescence turn-on effect, the corresponding taxoid−pyrazolines **1a**−**4a** were purified to homogeneity and their photophysical properties were measured along with those of taxoid−tetrazoles **1**−**4** (Figures S5−S10). As shown in Table 1, the *N*, *N*-dihydroxyethylamino substituted taxoid−tetrazoles (**1** and **2**) showed a bathochromic shift in $\lambda_{max}$ compared to the glycolamide substituted ones (**3** and **4**) in acetonitrile (ACN)/PBS buffer (1:1), consistent with what we observed previously.[19] However, taxoid−tetrazoles **3** and **4** showed higher coefficients at their $\lambda_{max}$. On the other hand, the taxoid−pyrazolines showed significant bathochromic shift, with $\lambda_{max}$ ranging from 330 to 358 nm. Whereas none of the taxoid−tetrazoles was fluorescent, broad emission spectra were obtained for all taxoid−pyrazolines, with $\lambda_{em}$ ranging from 528 nm for **4a** to 617 nm for **1a**. The fluorescent properties of taxoid−pyrazolines appeared to be solvent-dependent; for example, the fluorescence quantum yields of **1a** and **2a** jumped from 0.0024 and 0.0041 in ACN-mixed PBS buffer to 0.036 and 0.022 in DCM, respectively (compare Figure S6 to S5; Figure S8 to S7). Interestingly, taxoid−pyrazolines **3a** and **4a** exhibited significantly higher fluorescence quantum yields in ACN/PBS buffer (1:1), with $\Phi_F$ values to be 0.034 and 0.056, respectively. Because of the difference in their brightness, the four taxoid−tetrazoles showed varying degrees of fluorescence turn-on effect, ranging from 21-fold for photoactivation of **1** to 112-fold for photoactivation of **4** in ACN/PBS buffer (1:1) (Table 1).

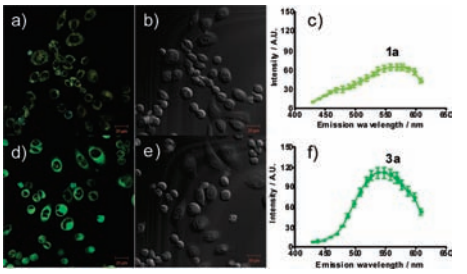


**Figure 1.** Confocal spectrum-scan micrographs of taxoid−pyrazoline labeled microtubules in live CHO cells. CHO cells were treated with 1 μM of taxoid−pyrazoline **1a** (a and b) or **3a** (d and e) for 30 min and the fluorescence spectrum-scan in the region of 428−608 nm (a and d) and the corresponding DIC images (b and e) were recorded with a Zeiss LSM 710 microscope; $\lambda_{ex}$ = 405 nm. The colors rendered in the fluorescence micrographs were λ-encoded (real color). Scale bar = 20 μm. The average intensities of the unsaturated fluorescence-labeled cytoskeleton areas in 10 selected cells were plotted to give the in-cell fluorescence spectrum of **1a** (c) or **3c** (f) along with the standard deviations.

It is known that the modification of paclitaxel on position-7 does not affect its binding to β-tubulins,[16] the building blocks for polymeric microtubules. To investigate whether this is also true for our pyrazoline-modified taxoids, HeLa cells were treated with 5 μM of preactivated taxoid−pyrazoline **1a** for 30 min. After cell fixation and permeabilization, the binding of taxoid−pyrazoline **1a** to microtubules was confirmed by confocal fluorescence microscopy in which the distribution of pyrazoline fluorescence overlaid nicely with that of an Alexa Fluor-568 based immunostain for microtubules (Figure S11). Conversely, since the binding of taxoid to β-tubulins may bring the hydrophobic pyrazoline fluorophores to the microtubule surface, it is also possible that the photophysical properties of taxoid−pyrazolines may be altered. To probe this possibility, CHO cells were treated with 1 μM of the preactivated taxoid-pyrazolines **1a**−**4a** for 30 min, and the taxoid−pyrazoline fluorescence upon binding to microtubules was examined with a spectrum-scan confocal microscope. To our surprise, among the four taxoid−pyrazolines, compounds **1a** and **3a** showed moderate and strong fluorescent labeling of microtubules, respectively (Figure 1), while compounds **2a** and **4a** showed very weak intracellular fluorescence (Figure S12). This drastic difference in fluorescent properties apparently is dependent on the linker length; the long flexible linkers such as those in **2a** and **4a** (Scheme 1) possibly position the pyrazoline fluorophores in a protein environment where their fluorescences are quenched. A closer examination of in-cell fluorescence spectra revealed that the peak emission wavelengths have shifted from 617 to around 569 nm for **1a** (Figure 1c), and from 584 to 543 nm for **3a** (Figure 1f). These hypsochromic shifts are presumably due to the interactions of the pyrazoline fluorophores with the microtubule surface, and have been observed previously for the fluorescein-conjugated taxols.[16b] As expected,

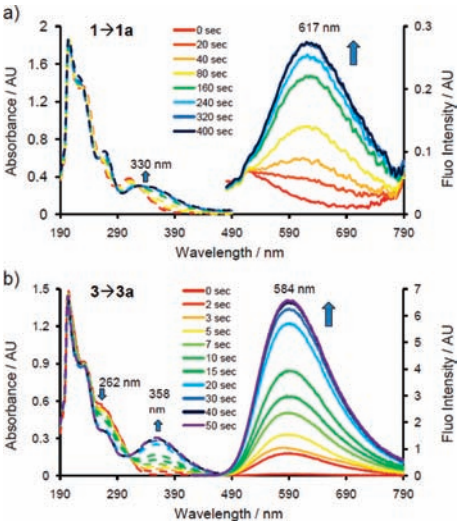


**Figure 2.** Time courses of photoactivation of taxoid−tetrazoles **1** (a) and **3** (b) as monitored by UV−vis (dashed lines) and fluorescence (solid lines). Compounds were dissolved in acetonitrile/PBS (1:1) to derive concentrations of 25 $\mu$M, and the photoirradiation wavelengths were set at 365 nm for **1** and 302 nm for **3**. For fluorescence, $\lambda_{ex}$ = 405 nm.

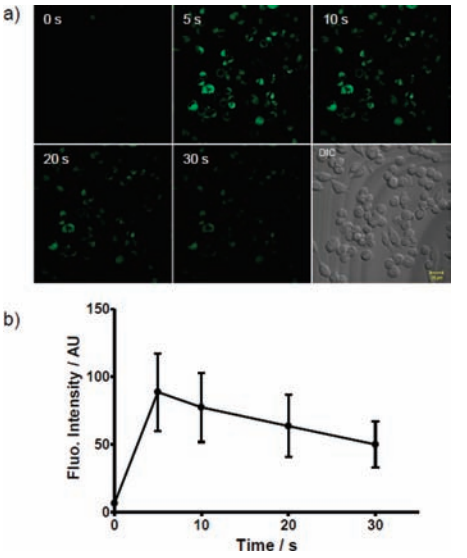


**Figure 3.** Time course of the photoactivation of taxoid−tetrazole **3** in live CHO cells. (a) Time-lapsed confocal micrographs of tetrazole-treated CHO cells after photoillumination, scale bar = 20 $\mu$m. Cells were treated with 1 $\mu$M of taxoid−tetrazole **3** for 30 min before photoillumination. ZEISS filter set #49 was used for incident light filtering; for fluorescence, $\lambda_{ex}$ = 405 nm. (b) Plot of the changes of fluorescence of **3a** over a period of 30 s. For each time point, the fluorescence intensities inside the cytosols of 10 individual cells with unsaturated fluorescence were used in the calculation of the averaged intensities and the standard deviations.

taxoid−pyrazoline **3a** is a brighter fluorescent probe than **1a** as it showed a higher fluorescence intensity inside CHO cells.

On the basis of the in-cell spectrum scan results, taxoid−tetrazoles **1** and **3** were selected and their photoactivation kinetics in vitro were examined (Figure 2). Because taxoid−tetrazole **1** showed broad absorption, we carried out the photoactivation using a 365 nm hand-held UV lamp (3.5 mW/cm$^2$). Figure 2a shows that a complete conversion to the desired taxoid−pyrazoline **1a** was achieved in 320 s, as evidenced by the gradual increase in a new absorption band centered at 330 nm and a broad emission band centered at 617 nm. On the other hand, since taxoid−tetrazole **3** showed almost no absorption at 365 nm, it was subjected to 302 nm photoirradiation (2.3 mW/cm$^2$). Gratifyingly, complete conversion to fluorescent taxoid−pyrazoline **3a** was achieved in 40 s, with the pyrazoline product showing an absorption band at 358 nm and a strong emission band at 584 nm (Figure 2b). Overall, these two taxoid−tetrazoles offer complementary features as photoactivatable turn-on fluorophores: tetrazole **3** exhibits robust turn-on effect and higher brightness, while tetrazole **1** can be activated with long-wavelength light (365 nm), which makes it potentially suitable for laser-scanning fluorescence microscopy studies with improved spatiotemporal resolution.

To examine whether taxoid−tetrazoles can be photoactivated in vivo, CHO cells were treated with 1 $\mu$M of taxoid−tetrazole **3** for 30 min, and after washing with prewarmed PBS three times, the treated cells were illuminated continuously with a metal halide light source (EXFO-XCite, 25% of 13.3 mW/cm$^2$) through a filter with bandwidth of 300/395 nm, and the in situ formed taxoid−pyrazoline fluorescent signals were recorded with an acquisition window of 535−545 nm. A rapid, roughly 12-fold increase in fluorescence in the CHO cytosols was detected after 5-s photoirradiation (compare fluorescence intensity at 5 s to background fluorescence at 0 s; Figure 3). By comparing the fluorescence intensity at 5 s to the maximal intensity for the taxoid−pyrazoline **3a** (Figure 1f), a calculated 79% yield was derived for the photoactivation in vivo. The fluorescence intensities decreased over extended photoirradiation; however, 56% of fluorescence signals still remained after 30 s photoirradiation, indicating that the pyrazoline fluorophore **3a** is fairly resistant to photobleaching. The photobleaching rate of **3a** was similar to that of DAPI measured under identical microscopic conditions (Figure S13).

Since taxoid−tetrazole **1** shows 365-nm photoactivatability and its UV−vis absorption extends to 405 nm (albeit weak), a laser wavelength available in our microscope, we decided to examine whether photoactivation can be carried out with the 405-nm laser, which would allow a spatiotemporal control over the in situ fluorescence generation. Thus, CHO cells were treated with 10 $\mu$M taxoid−tetrazole **1** for 30 min and then washed with prewarmed PBS three times. Then, a select subpopulation of cells in the optical field (area outlined in red rectangle in Figure 4) was subjected to a brief (11 s) 405-nm diode laser irradiation (30 mW) at 100% power while the cells outside the selected area were not. Afterward, the entire population was scanned for fluorescence emissions with excitation at 405 nm at 20% power. Strong turn-on fluorescence was detected for cells within the rectangular area, in sharp contrast to the weak fluorescence background for cells outside the activation area (Figure 4). Quantification of cytosolic fluorescence intensity in CHO cells revealed a 7-fold enhancement in fluorescence for the activated cells relative to the unactivated cells. With this photoactivatable microtubule fluorescent probe, in principle it should be possible in the future to label microtubules asymmetrically within a single cell and identify factors that break cellular symmetry during the cell division.[21]

In conclusion, we have demonstrated a new strategy for designing turn-on fluorescent probes in which a protein-targeting core is linked to a photoactivatable, alkene-appended tetrazole. Using the tetrazole-modified taxoids as a model, robust fluorescence turn-on (up to 112-fold) was observed within ~1 min after

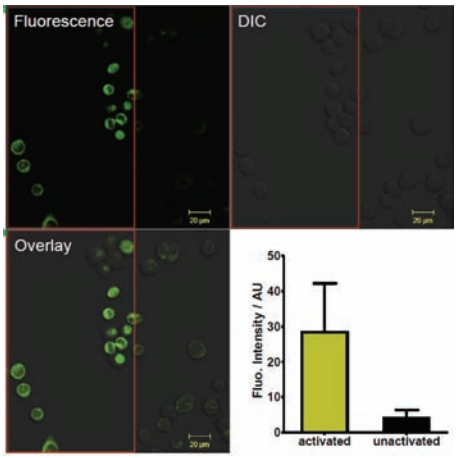


**Figure 4.** Spatially controlled photoactivation of taxoid−tetrazole **1** in CHO cells. Cells were treated with 10 $\mu$M taxoid−tetrazole **1** for 30 min and then washed three times with prewarmed PBS. Cells in the red rectangle area were exposed to 405-nm laser at 30 mW for 11 s followed by fluorescence acquisition, $\lambda_{ex}$ = 405 nm. For confocal micrographs, scale bar = 20 $\mu$m. For the plot, the fluorescence intensities from the cytosols of all the activated cells inside the red rectangle area were quantified using ImageJ program and compared to those of the unactivated cells.

the intramolecular photoclick reaction under the 302 nm photoirradiation in ACN/PBS buffer (1:1). Two taxoid−tetrazoles with short linkers, **1** and **3**, showed extremely fast photoinduced cycloaddition inside living cells (in seconds), producing strong pyrazoline fluorescent probes in situ for cytosolic microtubules. Moreover, **1** can be activated using 405 nm laser as the photoactivation light source, enabling a spatially controlled fluorescent labeling of microtubules in living cells. Compared to the photouncaging approach, this photoclick chemistry based approach produces $N_2$ as the only side product, which is nontoxic to cells. Also, the fluorescent properties of the resulting pyrazoline fluorophores are highly tunable,[22] for example, through the appendage of other alkene dipolarophiles. By employing a 'scaffold hopping' strategy[23] we reported recently, it should be possible to further improve the photoactivation efficiency, for example, by increasing absorption at 405 nm through the use of other aromatic scaffolds, and obtain turn-on pyrazoline fluorophores with increased brightness and photostability.

## ■ ASSOCIATED CONTENT

**Supporting Information.** Supplemental figures, synthetic schemes and experimental procedures, confocal micrographs, and characterization of all compounds. This material is available free of charge via the Internet at http://pubs.acs.org.

## ■ AUTHOR INFORMATION

**Corresponding Author**
qinglin@buffalo.edu

## ■ ACKNOWLEDGMENT

We gratefully acknowledge the NIH (R01 GM 085092) for financial support, Alan Siegel at the SUNY Buffalo Biological Sciences Imaging Facility for assistance in microscopy, and the National Science Foundation Major Research Instrumentation grant (DBI-0923133) for instrumentation support.

## ■ REFERENCES

(1) Fernandez-Suarez, M.; Ting, A. Y. *Nat. Rev. Mol. Cell Biol.* **2008**, *9*, 929.
(2) Folling, J.; Belov, V.; Kunetsky, R.; Medda, R.; Schonle, A.; Egner, A.; Eggeling, C.; Bossi, M.; Hell, S. W. *Angew. Chem., Int. Ed.* **2007**, *46*, 6266.
(3) Krafft, G. A.; Sutton, W. R.; Cummings, R. T. *J. Am. Chem. Soc.* **1988**, *110*, 301.
(4) Zhao, Y.; Zheng, Q.; Dakin, K.; Xu, K.; Martinez, M. L.; Li, W. H. *J. Am. Chem. Soc.* **2004**, *126*, 4653.
(5) Gee, K. R.; Weinberg, E. S.; Kozlowski, D. J. *Bioorg. Med. Chem. Lett.* **2001**, *11*, 2181.
(6) Zheng, G.; Guo, Y. M.; Li, W. H. *J. Am. Chem. Soc.* **2007**, *129*, 10616.
(7) Maurel, D.; Banala, S.; Laroche, T.; Johnsson, K. *ACS Chem. Biol.* **2010**, *5*, 507.
(8) Hu, D.; Tian, Z.; Wu, W.; Wan, W.; Li, A. D. Q. *J. Am. Chem. Soc.* **2008**, *130*, 15279.
(9) Keating, A. E.; Garcia-Garibay, M. A. In *Organic and Inorganic Photochemistry*; Ramamurthy, V., Schanze, K., Eds.; Marcel Dekker: New York, 1998; Vol. 2; pp 195−248 and references therein.
(10) Betzig, E.; Patterson, G. H.; Sougrat, R.; Lindwasser, O. W.; Olenych, S.; Bonifacino, J. S.; Davidson, M. W.; Lippincott-Schwartz, J.; Hess, H. F. *Science* **2006**, *313*, 1642.
(11) Rust, M. J.; Bates, M.; Zhuang, X. *Nat. Methods* **2006**, *3*, 793.
(12) Lee, H. L.; Lord, S. J.; Iwanaga, S.; Zhan, K.; Xie, H.; Williams, J. C.; Wang, H.; Bowman, G. R.; Goley, E. D.; Shapiro, L.; Twieg, R. J.; Rao, J.; Moerner, W. E. *J. Am. Chem. Soc.* **2010**, *132*, 15099.
(13) (a) Song, W.; Wang, Y.; Qu, J.; Lin, Q. *J. Am. Chem. Soc.* **2008**, *130*, 9654. (b) Wang, Y.; Song, W.; Hu, W. J.; Lin, Q. *Angew. Chem., Int. Ed.* **2009**, *48*, 5330. (c) Song, W.; Wang, Y.; Yu, Z.; Vera, C. I.; Qu, J.; Lin, Q. *ACS Chem. Biol.* **2010**, *5*, 875. (d) Song, W.; Yu, Z.; Madden, M. M.; Lin, Q. *Mol. BioSyst.* **2010**, *6*, 1576.
(14) Desai, A.; Mitchison, T. J. *Annu. Rev. Cell Dev. Biol.* **1997**, *13*, 83.
(15) (a) Nicolaou, K. C.; Dai, W. M.; Guy, R. K. *Angew. Chem., Int. Ed.* **1994**, *33*, 15. (b) Yvon, A. M. C.; Wadsworth, P.; Jordan, M. A. *Mol. Biol. Cell* **1999**, *10*, 947.
(16) (a) Souto, A. A.; Acuña, U.; Andreu, J. M.; Barasoain, I.; Abal, M.; Amat-Guerri, F. *Angew. Chem., Int. Ed.* **1995**, *34*, 2710. (b) Díaz, J. F.; Strobe, R.; Engelborghs, Y.; Souto, A. A.; Andreu, J. M. *J. Biol. Chem.* **2000**, *275*, 26265.
(17) Guy, R. K.; Scott, Z. A.; Sloboda, R. D.; Nicolaou, K. C. *Chem. Biol.* **1996**, *3*, 1021.
(18) Light energy was measured by placing a FieldMaster GS energy analyzer equipped with LM-10 HTD power meter sensor 2-cm away from the lamp.
(19) Wang, Y.; Hu, W. J.; Song, W.; Lim, R. K. V.; Lin, Q. *Org. Lett.* **2008**, *10*, 3725.
(20) (a) Du, H.; Fuh, R. C. A.; Li, J.; Corkan, L. A.; Lindsey, J. S. *Photochem. Photobiol.* **1998**, *68*, 141. (b) Hard, T.; Fan, P.; Kearns, D. R. *Photochem. Photobiol.* **1990**, *51*, 77.
(21) Mullins, R. D. *Cold Spring Harbor Perspect. Biol.* **2010**, *2*, a003392.
(22) Fahrni, C. J.; Yang, L.; Van Derveer, D. G. *J. Am. Chem. Soc.* **2003**, *125*, 3799.
(23) Yu, Z.; Ho, L. Y.; Wang, Z.; Lin, Q. *Bioorg. Med. Chem. Lett.* **2011**. DOI: 10.1016/j.bmcl.2011.04.087.